The Astrophysical Journal Letters, 818:L5 (6pp), 2016 February 10 doi:10.3847/2041-8205/818/1/L5

EVENTS LEADING UP TO THE 2015 JUNE OUTBURST OF V404 CYG

F. Bernardini[1,2], D. M. Russell[1], A. W. Shaw[3], F. Lewis[4,5], P. A. Charles[3,6], K. I. I. Koljonen[1], J. P. Lasota[7,8], and J. Casares[9,10,11]
[1] New York University Abu Dhabi, P.O. Box 129188, Abu Dhabi, United Arab Emirates; bernardini@nyu.edu
[2] INAF—Osservatorio Astronomico di Capodimonte, Salita Moiariello 16, I-80131 Napoli, Italy
[3] Department of Physics & Astronomy, University of Southampton, Southampton SO17 1BJ, UK
[4] Faulkes Telescope Project, School of Physics & Astronomy, Cardiff University, The Parade, CF24 3AA, Cardiff, Wales
[5] Astrophysics Research Institute, Liverpool John Moores University, 146 Brownlow Hill, Liverpool L3 5RF, UK
[6] ACGC, University of Cape Town, Private Bag X3, Rondebosch, 7701, South Africa
[7] Institut d'Astrophysique de Paris, CNRS et Sorbonne Universités, UPMC Paris 06, UMR 7095, 98bis Bd Arago, F-75014 Paris, France
[8] Nicolaus Copernicus Astronomical Center, Bartycka 18, 00-716 Warsaw, Poland
[9] Instituto de Astrofísica de Canarias, E-38205 La Laguna, Santa Cruz de Tenerife, Spain
[10] Departamento de Astrofísica, Universidad de La Laguna, E-38206 La Laguna, Santa Cruz de Tenerife, Spain
[11] Department of Physics, Astrophysics, University of Oxford, Denys Wilkinson Building, Keble Road, Oxford OX1 3RH, UK
Received 2016 January 14; accepted 2016 January 16; published 2016 February 2

ABSTRACT

On 2015 June 15 the burst alert telescope (BAT) on board *Swift* detected an X-ray outburst from the black hole (BH) transient V404 Cyg. We monitored V404 Cyg for the last 10 years with the 2-m Faulkes Telescope North in three optical bands (V, R, and i'). We found that, one week prior to this outburst, the optical flux was 0.1–0.3 mag brighter than the quiescent orbital modulation, implying an optical precursor to the X-ray outburst. There is also a hint of a gradual optical decay (years) followed by a rise lasting two months prior to the outburst. We fortuitously obtained an optical spectrum of V404 Cyg 13 hr before the BAT trigger. This too was brighter than quiescence, and showed spectral lines typical of an accretion disk, with characteristic absorption features of the donor being much weaker. No He II emission was detected, which would have been expected had the X-ray flux been substantially brightening. This, combined with the presence of intense Hα emission, about seven times the quiescent level, suggests that the disk entered the hot, outburst state before the X-ray outburst began. We propose that the outburst is produced by a viscous–thermal instability triggered close to the inner edge of a truncated disk. An X-ray delay of a week is consistent with the time needed to refill the inner region and hence move the inner edge of the disk inwards, allowing matter to reach the central BH, finally turning on the X-ray emission.

Key words: accretion, accretion disks – black hole physics – X-rays: individual (V404 Cyg, GS 2023+338)

1. INTRODUCTION

In low mass X-ray binaries (LMXBs) a black hole (BH) or a neutron star (NS) accretes matter from a low mass ($M \sim M_{\odot}$) Roche lobe filling companion. Many LMXBs are transient, alternating between long periods of quiescence (years), where the X-ray luminosity is faint ($\leqslant 10^{33}$ erg s^{-1}) to shorter episodes of outburst where the X-ray luminosity strongly increases (10^{37-38} erg s^{-1}) and can approach the Eddington limit.

Coriat et al. (2012) showed that the global behavior of LMXB outbursts is well described by the thermal–viscous disk instability model (DIM; see, e.g., Cannizzo 1993; Lasota 2001), where in quiescence a cold, non-stationary disk fills-up with matter until at some radius its temperature having reached a critical value triggers an outburst. Heating fronts propagate through the disk bringing it to a hot, quasi-stationary, bright state at which the X-ray luminosity reaches its maximum. The DIM can broadly explain the LMXB outburst cycle only if the inner disk is truncated during quiescence (Dubus et al. 2001, hereafter DHL).

The accretion flow structure inside the truncated disk's hole during quiescence forms a hot, optically thin, radiatively inefficient plasma (see e.g., Narayan et al. 1997; Narayan & McClintock 2008) that shines in X-rays, and/or a jet (Hynes et al. 2009; Xie et al. 2014), while the outer disk remains cool. However, from a DIM perspective the inner flow is not important, as long as it does not contribute to the dynamics of the disk (DHL).

V404 Cyg (=GS 2023+338), hereafter V404, is one of the closest and best studied LMXBs (2.39 ± 0.14 kpc; Miller-Jones et al. 2009). It hosts a $9 \pm^{0.2}_{0.6}$ $M_{\odot}$ BH (Khargharia et al. 2010) with an orbital period of 6.4714 ± 0.0001 days (Casares & Charles 1994). V404 showed at least three outbursts (1938, 1956, and 1989; Makino 1989; Richter 1989; Życki et al. 1999), now followed by the burst alert telescope (BAT; Barthelmy et al. 2005) triggering on V404 on 2015 June 15 18:31:38 UT (MJD 57188.772; Barthelmy et al. 2015) when the first X-ray flare of a new outburst was detected, followed by multiple flares in hard X-rays with fast rise time and durations of hours (Rodriguez et al. 2015).

An optical precursor of the first X-ray flare was detected with the 2-m Faulkes Telescope North (FTN) a week before the first BAT trigger (Bernardini et al. 2015). Due to the sporadic nature of LMXB outburst start times, to the small number of transient sources currently known, and to the lack of regular high signal-to-noise ratio (S/N) monitoring (nowadays difficult at X-ray wavelengths but easier at optical wavelengths), it is hard to detect a delay in the rise to outburst between short (X-ray) and long (IR–optical) wavelengths.

Only five other sources have shown an indication of similar behavior (Orosz et al. 1997; Shahbaz et al. 1998; Jain et al. 2001; Wren et al. 2001; Uemura et al. 2002; Buxton & Bailyn 2004; Zurita et al. 2006). This X-ray delay of uncertain origin, is reminiscent of the well-documented dwarf-nova outbursts UV to optical delay (Smak 1998, and references therein). However, the above LMXBs during quiescence were

fainter than the detection limit of X-ray instruments, so their X-ray emission could have started rising well before the first X-ray detection (the derived X-ray delay could be much lower than reported).

We monitored V404 with the 2-m FTN since 2006 and report here on the detailed analysis of the optical light curves from 2006 up to the time of the BAT trigger, and on the optical spectrum of V404 fortuitously collected with the William Herschel Telescope (WHT) ∼13 hr before the trigger. This is the closest in time an optical spectrum of an LMXB has been acquired prior to its first X-ray outburst detection. We discuss the results in the framework of the DIM (DHL).

2. OBSERVATIONS AND DATA REDUCTION

2.1. Optical Photometry

Observations of V404 were taken with the 2-m FTN (Haleakala, Maui, USA). Imaging was obtained in Bessell V, Bessell R, and Sloan Digital Sky Survey i' filters since 2006 April, as part of a monitoring campaign of ∼40 LMXBs (Lewis et al. 2008). We present more than nine years of data (from 2006 April 8 to 2015 June 9). Observations were typically made once per week when V404 was visible, and exposure times are 200 s in each filter. Automatic pipelines de-bias and flat-field the FTN science images.

There is a field star of magnitude $V = 18.90 \pm 0.02$, $R = 17.52 \pm 0.01$, $i' = 16.92 \pm 0.01$ just 1.4 arcsec north of V404 (Udalski & Kaluzny 1991; Casares et al. 1993; Barentsen et al. 2014). The two stars are blended in all images, so we performed aperture photometry (using PHOT in IRAF) adopting an optimum fixed aperture radius of 12 pixels (3.″6) to encompass the flux of both stars. The same aperture was used for photometry on four comparison stars 13–34 arcsec from V404. These were used for flux calibration, and themselves calibrated using field stars of known magnitudes listed in Udalski & Kaluzny (1991) for V-band, Casares et al. (1993) for R-band and the second data release of the IPHAS (INT Photometric Hα Survey of the Northern Galactic Plane catalog; Barentsen et al. 2014) for i'. Magnitudes of V404 were obtained in total from 392 usable images.

2.2. Optical Spectroscopy

V404 was observed on 2015 June 15 at UTC 0500 (MJD 57188.208) with the Intermediate dispersion Spectroscopic and Imaging System (ISIS) on the 4.2-m WHT at Observatorio del Roque de Los Muchachos, La Palma, Spain. We obtained two 600 s exposures covering a total spectral range 4173–7153 Å, utilizing the R600B and R gratings and a 1″ slit in photometric conditions of good (∼1″) seeing. Spectra were reduced and extracted using standard IRAF procedures. The one-dimensional spectra were wavelength calibrated using a low-order polynomial fit to the pixel-wavelength arc data. We flux-calibrated the spectrum using the nearby flux standard star BD +25 4655 (Oke 1990). The WHT observations were previously reported in Muñoz-Darias et al. (2015).

3. RESULTS

3.1. X-Ray Rise to Outburst

We convert the BAT 15–50 keV count rate averaged on each orbit (Krimm et al. 2013) at the time of trigger (MJD 57188.772) and the first 3σ upper limit before the trigger (MJD 57188.705) to unabsorbed 15–50 keV flux using WebPIMMS. Since the spectrum of the first flare is highly absorbed and the spectral shape not well constrained, we used a power law with slope $\Gamma = 0.3$–1.2 (Kuulkers et al. 2015). We measure $F = 4.0 \pm 0.5 \times 10^{-8}$ erg cm^{-2} s^{-1} and $F < 4.2 \times 10^{-9}$ erg cm^{-2} s^{-1}, respectively. V404 displays X-ray variability a factor of a few in quiescence (Bernardini & Cackett 2014). We convert the lowest literature X-ray quiescent 0.3–10 keV flux (2006 *XMM-Newton* pointing; Bradley et al. 2007) to 15–50 keV flux using WebPIMMS, $\Gamma = 1.85$ and $N_H = 1 \times 10^{22}$ cm^{-2} (Rana et al. 2015), and obtain $F \sim 1 \times 10^{-12}$ erg cm^{-2} s^{-1}. Assuming that the rise to outburst of the first X-ray flare was monotonic and slow, e.g., a single exponential rise starting from the quiescent level or above it, it must have begun after MJD 57188.530.

The flares detected by *INTEGRAL* (Winkler et al. 2003) at 25–100 keV after the BAT trigger show a fast rise ($\lesssim$1 hr) and duration of hours (Rodriguez et al. 2015). Moreover, during its 1989 outburst, the 1.2–37 keV light curve of V404 showed flares with very fast rises (minutes; Kitamoto et al. 1989; Terada et al. 1994; Życki et al. 1999). A complex behavior for the X-ray rise to outburst, e.g., a slow rise followed by a sudden increase, cannot be excluded since the source in quiescence is below the BAT detection limit. We conclude that MJD 57188.53 can be safely considered as a lower limit to the rise to outburst of the first X-ray flare detected by BAT.

3.2. Optical Photometry

In Figure 1 we show the optical light curve in V, R and i' bands, from 2006 up to the 2015 BAT trigger. A week before it (the last two points), the V, R and i' magnitudes are the highest recorded throughout this time.

Using $P_{\rm orb} = 6.4714 \pm 0.0001$ day and $T_0 = 2448813.873 \pm 0.004$ HJD as orbital ephemerides (Casares & Charles 1994), we generate the orbital light curve (Figure 2). The relative uncertainty on the phase determined with these ephemerides is ∼0.05, across the entire duration of our observations, but only ∼0.005 from one year to the next. The typical variation due to the tidally distorted donor's ellipsoidal modulation is present. Low amplitude flaring, likely due to residual accretion activity, is also present, as has been documented before (Shahbaz et al. 2003; Hynes et al. 2004, 2009; Zurita et al. 2004; Bernardini & Cackett 2014).

We fit the orbital light curves (except the last two points) with a constant plus double sinusoid function, whose phases are free to vary so as to account for unequal minima and maxima, as frequently seen in quiescent LMXBs including V404 (Zurita et al. 2004). On 2015 June 8 (MJD ∼ 57181.5, $\phi \sim 0.11$), and 9 (MJD ∼ 57182.5, $\phi \sim 0.25$) the optical magnitude in all bands is significantly brighter than the average quiescent modulation level by 0.1–0.3 mag, and above the low amplitude flaring behavior (where Δ mag $\lesssim 0.1$). We subtract the best fitting model from the orbital light curves, and show in Figure 3 the residual light curves. We note that the last two points of the light curves have the highest residuals, that the residuals in the different bands look correlated on short timescales (days) and that a long-term trend (years) seems present (first a decay and then a rise).

We measure the statistical significance of the correlation using Spearman's rank test on the R and i' bands, where the S/N is higher compared to V. The Spearman's coefficient is $\rho = 0.78$, and the null hypothesis probability is

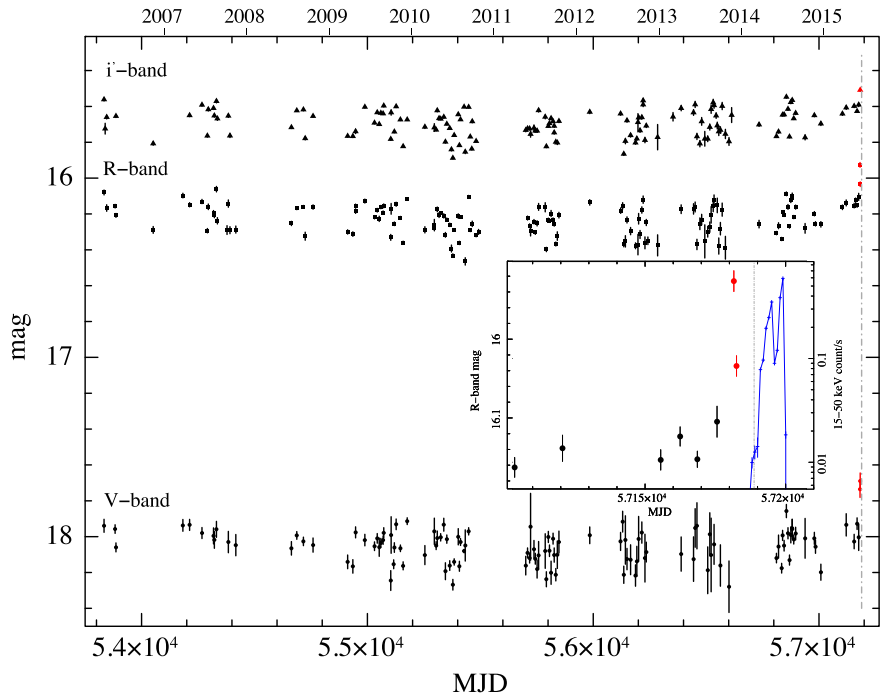

Figure 1. Optical light curve in i' (triangles), R (squares), and V (circles) band from 2006 to 2015. Magnitudes include flux from the nearby contaminating star. The dotted–dashed line at MJD 57188.772 shows the X-ray trigger. The red points are 2015 June 8 (MJD 57181.5) and 9 (MJD 57182.5). No observation in i' band was performed on 2015 June 8. In the insert, a zoom-in of the 2015 R band data compared with the 3σ BAT detections (blue crosses).

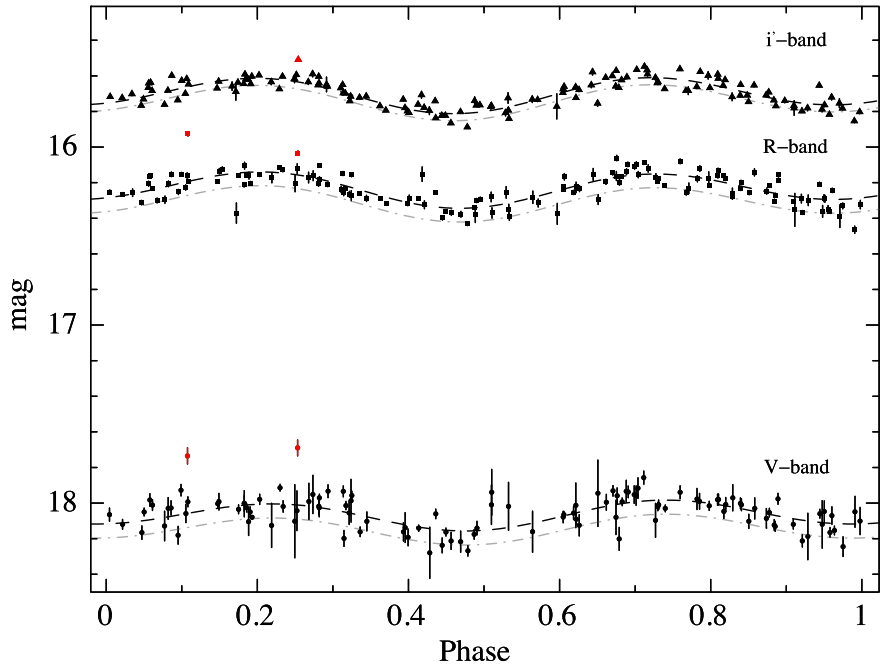

Figure 2. Orbital light curves. The dashed line is a constant plus two sines best fitting model. The dotted–dashed line is the lower envelope.

$P = 3.5 \times 10^{-27}$, so the residuals are positively correlated. This and the small error bars on each data point, suggest that the observed variability is intrinsic to the source and is likely accretion activity on timescales longer than minutes (the time between two consecutive exposures). We combine the i' and R band residuals. In the bottom panel of Figure 3 we show the average of R and i' bands, $\langle \Delta i', \Delta R \rangle = 0.5(\langle \Delta i' \rangle + \langle \Delta R \rangle)$, where we use three points per bin. The decreasing–increasing trend is now clearer. We fit the first part of the light curve (up to MJD 55834.5) with a constant plus a linear function. An F-test gives a 4.4σ significance for the inclusion of the latter. Between MJD 53860 and 55834.5 we measure a decrease of $\sim$0.02 mag yr^{-1}.

We detect an optical precursor to the first X-ray flare registered by BAT. Assuming that the two events are directly linked and that the rise of the X-ray flare is monotonic, we estimate a delay in the rise of the X-ray (MJD $\sim$ 57188.5) compared to the optical (MJD $\sim$ 57181.5) emission of at least 7

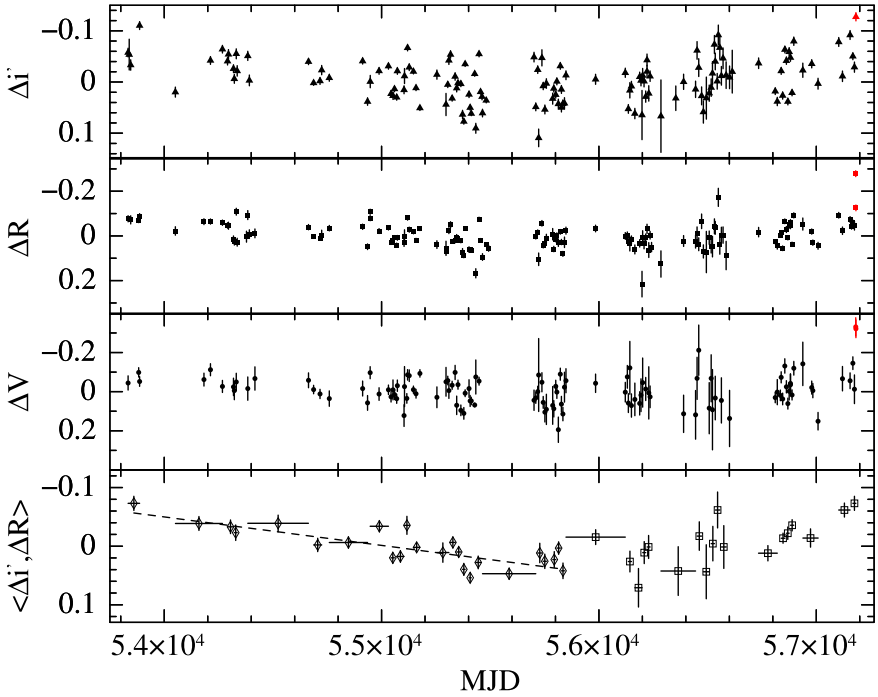

Figure 3. Residual light curves. The bottom panel shows the average of the residual in the i' and R band. The dashed line is a fit made with a constant plus a linear component.

days. It could be as long as 13 days, considering that the optical flux may have started rising immediately after the pointing before the precursor (MJD ∼ 57175.6). The delay's length is similar to those seen in the other four LMXBs that showed indication of this behavior. We have also found evidence of a long-term trend. The last two points of the residual light curve before the outburst are significantly above this quiescent downward trend. Consequently, we can constrain the long-term rise to have started before MJD 57129.5 (2015 April 17).

3.3. Spectral Energy Distribution (SED)

To construct the SED of the optical precursor, we first measure the lower envelope of the modulation (see Zurita et al. 2004), which is the donor contribution at each phase (Figure 2). We combine the 2015 June 8 and 9 images (in the i' band only June 9 is available), and we subtract the lower envelope from the derived magnitudes. We de-redden the fluxes of the residuals using $A_V = 4$ (Casares et al. 1993; Hynes et al. 2009) and the extinction law of Cardelli et al. (1989), and measure a precursor spectral index $\alpha = -0.35 \pm 0.32$, where $F_\nu \propto \nu^\alpha$. This is consistent with a 7500 ± 1500 K blackbody, which peaks in the visible. These errors do not take into account any uncertainties in the extinction A_V (Hynes et al. 2009).

The SED could be consistent, within 1σ confidence level, with both optically thin synchrotron emission with $\alpha \sim -0.7$, or optically thick (flat) synchrotron emission with $\alpha \sim 0$. However, Bernardini et al. (2016) showed that during the 1989 outburst the jet dominates the optical flux in the hard state, but makes marginal contribution in quiescence.

We measured a de-reddened spectral index from the WHT spectrum of $\alpha = -1.85 \pm 0.08$ for the continuum, by removing the hydrogen lines from the red arm, similar to the spectral index of some flares seen during quiescence (Shahbaz et al. 2003); this suggests a variable spectrum during the initial rise into outburst.

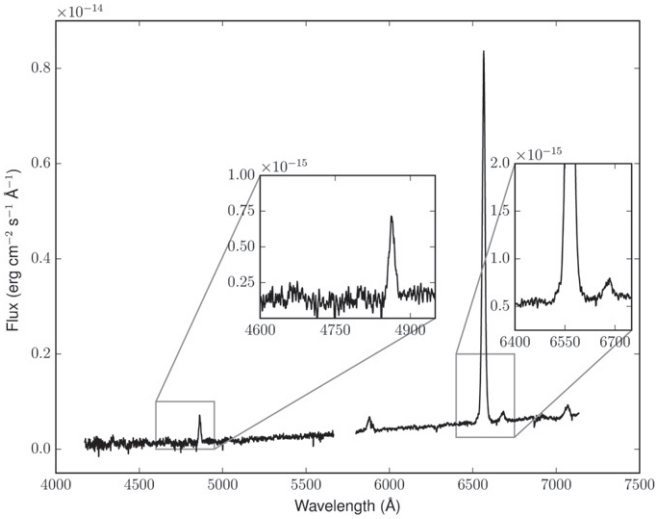

Figure 4. Averaged optical spectrum (smoothed using a 5-point boxcar algorithm) obtained with WHT/ISIS on 2015 June 15. The spectrum has been flux calibrated using the flux standard star BD+25 4655. The left and right insets show the zoomed in region around Hβ and the base of Hα, respectively.

3.4. Optical Spectroscopy

The optical spectrum is dominated by a strong Hα emission line (Figure 4). Hβ is also present, along with multiple He I emission lines. However, He II (4686 Å), typical of X-ray illuminated disks in outburst, is absent. At first sight the absorption features of the companion seem also absent, but a closer look reveals clear identifications hidden within the noise (Figure 5). A cross-correlation of the Hα pre-outburst spectrum and the average of 220 quiescent spectra of V404 obtained

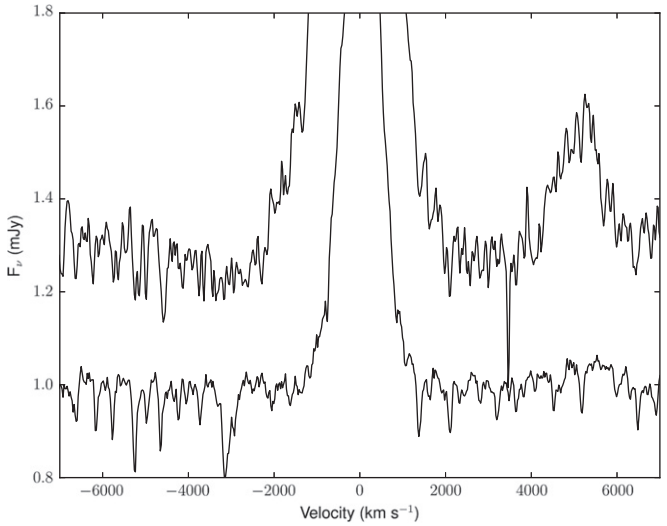

Figure 5. June 15 pre-outburst spectrum (offset by 0.3 mJy and smoothed with a Gaussian kernel of FWHM = 2 pixels) compared with the 20 year average quiescent spectrum (bottom), zoomed in on the region surrounding Hα. Spectra have been averaged in the rest frame of the companion.

between 1990 and 2009 (see Casares 2015) with the spectrum of the radial velocity template HR 8857 yields clear peaks at heliocentric velocities consistent with those of the donor star at the orbital phase of our spectra. The $\sim$7 $\times$ increase in Hα flux compared with the quiescent level (Casares & Charles 1992) suggests that the accretion disk is much brighter than in quiescence. We estimate the inner radius of the truncated disk, $R_{\rm in} = 0.5(c\,\sin(i)/v_{\rm in})^2$, by studying H$\alpha$ in emission. By measuring its half-width at zero intensity (HWZI) we estimate the velocity at the inner edge of the disk $v_{\rm in}$ (Narayan et al. 1996). We use a nonlinear least squares algorithm to fit a low-order polynomial to the continuum (masking Hα) and subtracting it. We apply the same approach to fit a double Gaussian to the Hα profile, finding it more accurate than a single Gaussian due to a broader component being present at the base of the line (Figure 4). We utilize the lower amplitude broader Gaussian to estimate the HWZI and hence $v_{\rm in}$ by measuring 5σ.

From fits to the lower amplitude broad Gaussian we find a slightly redshifted Hα peak at 6564.3 $\pm$ 0.1 Å with HWZI = 54.0 $\pm$ 0.5 Å, which translates to $v_{\rm in} = 2468 \pm 23$ km s^{-1}. This is actually a lower limit on $v_{\rm in}$, as higher velocity structure is present around the base of the line profile, though difficult to fit. Using the derived inclination of $i = 67^\circ$ (Khargharia et al. 2010) we find that $R_{\rm in} < 6200$ Schwarzschild radii ($R_s = 2GM_{\rm BH}/c^2$) at MJD 57188.208.

For comparison, the HWZI of the average quiescence Hα line has HWZI $\lesssim$ 1500 km s^{-1}, implying $R_{\rm in} \gtrsim$ 17,000 R_s. Therefore, the inner disk radius may have decreased by a factor $\sim$3 in our pre-outburst spectrum with respect to quiescence.

4. DISCUSSION

The DIM predicts (see Equation (51) in Lasota 2001) that in LMXBs, only inside-out outbursts can occur (e.g., the instability is triggered well inside the accretion disk and will propagate outwards). Inside-out outbursts do not start exactly at the inner disk edge and fronts propagate both ways. To explain the long recurrence time and the intensity of the outbursts of LMXBs, and their quiescent X-ray luminosities, the DIM requires that the inner quiescent disk is truncated far from the compact object (DHL). The heating fronts propagate rapidly with a speed $\sim\alpha\, c_s$, where α is the the hot disk viscosity parameter and c_s the speed of sound. The in-going front dies out quickly reaching the truncation radius without affecting much of the disk structure and then the hole is refilled in a viscous time. Since the disk X-ray emission is mainly emitted in the disk inner regions, a delay of several days in the rise to outburst of the X-ray with respect to the optical emission is expected. In the case of a non-truncated disk the delay would be at most 1 day (DHL).

A description of the rise to outburst can be found in Section 5.1 of DHL. We discuss our results according to this latest version of the DIM. The delay represents the difference between the time t_V, when the outburst starts at some $R(V)$ of the truncated disk and the time t_X, when the moving-in inner disk edge reaches the radius $R(X)$, where $R(V) > R(X)$, attaining the temperature that allows emission of X-rays. The X-ray delay ($\Delta t_{\rm V-X}$) corresponds to the difference between the two radii. From Equation (16) of DHL we can estimate $R(V)$ if we assume that the 7 days X-ray delay corresponds to the viscous time ($t_{\rm vis} = \Delta t_{\rm V-X}$). We get $\Delta t_{\rm V-X} = 15.3\, M_{10}^{1/2}\alpha_{0.2}^{-1}T_5^{-1}(R_{10}^{1/2}(V) - R_{10}^{1/2}(X))$ days, where $M_{10} = M_{\rm BH}/10\,M_\odot$, $\alpha_{0.2} = \alpha/0.2$ is the hot branch viscosity parameter, $R_{10} = (R/10^{10}\,{\rm cm})$ is the disk radius, and $T_5 = (T/10^5\,{\rm K})$ is the midplane temperature, where $T \gtrsim$ 3–4 $\times$ 10^4 K at the start of the outburst (see Lasota et al. 2008). We use T = 30,000–50,000 K, α = 0.1–0.2, and $R(X) = 5 \times 10^8$ cm (as in DHL), and we derive that the instability corresponding to the outburst precursor (MJD 57181.5) may have been triggered at $R(V) \sim$ 0.9–2.2 $\times$ 10^9 cm ($\sim$340–830 R_s). We notice that the disk size is $\sim 10^{12}$ cm

We also derive a direct constraint on $R(V)$ from the HWZI of Hα. At MJD 57188.208, 13 hr before the first X-ray detection ($\sim$6.5 days after the optical precursor detection), $R(V) < 6200\,R_s$. This is an upper limit to $R(X)$, since $R(X) < R(V)$, and so it represents a constraint on the size of the inner edge of the truncated disk ($R_{\rm in}$), close to the X-ray outburst onset. We notice that this upper limit is consistent with $R(V)$ derived from DIM equations.

We can use Equation (A.1) in Lasota et al. (2008) to estimate the critical effective disk temperature ($T_{\rm eff}^+$) needed to ionize hydrogen and start the outburst. Using the derived $R_{\rm in}$, $T_{\rm eff}^+ \approx 7000$ K (the dependency on R, and M in the equation is weak). We note that at the time of the optical precursor the disk temperature (7500 $\pm$ 1500 K) is consistent with $T_{\rm eff}^+$.

All versions of the DIM predict a constantly increasing optical flux during quiescence (Lasota 2001), while observed quiescent fluxes of dwarf novae and LMXBs are constant or decreasing (however, see Wu et al. 2016). We observe a long-term trend in the optical magnitude of V404, a 0.1 mag decrease followed by a 0.1 mag increase. The source is known to show year-to-year optical modulation changes of similar intensity (see Figure 1 in Zurita et al. 2004). Most of the variability we detect above the orbital modulation is likely due to accretion activity and occurs at all orbital phases (Figure 2).

It is known that accretion is happening at a low level in quiescence (short term variability has been seen in X-ray, optical and radio). Small accretion rate changes from year to year, likely explain the long-term optical variations. The rise in the optical flux from 2015 April may reflect a recent increase in

$\dot{M}$ eventually culminating in the outburst. The disk becomes progressively hotter as matter builds up and when the temperature reaches the ionization level, the inside-out heating wave quickly propagates from the trigger site, close to the inner edge of the truncated disk, through the whole disk (in both directions). Then, the inner edge of the truncated disk moves inwards, on the longer viscous timescale, and a week after the optical precursor, when $R_{\rm in} < 6200\,R_s$ (a factor of ∼3 lower than in quiescence), it is hot enough to generate X-ray emission and we observe the first X-ray flare.

The FTN is maintained and operated by Las Cumbres Observatory Global Telescope Network. J.P.L. was supported by the CNES. J.C. acknowledges support by MINECO under grants AYA2013-42627 and PR2015-00397.

REFERENCES

Barentsen, G., et al. 2014, MNRAS, 444, 3230
Barthelmy, S. D., Barbier, L. M., Cummings, J. R., et al. 2005, SSRv, 120, 143
Barthelmy, S. D., D'Ai, A., D'Avanzo, P., et al. 2015, GCN, 17929
Bernardini, F., & Cackett, E. M. 2014, MNRAS, 439, 2771
Bernardini, F., Russell, D. M., & Lewis, F. 2015, ATel, 7761, 1
Bernardini, F., Russell, D. M., Koljonen, I. I., et al. 2016, ApJ, submitted
Bradley, C. K., Hynes, R. I., Kong, A. K. H., et al. 2007, ApJ, 667, 427
Buxton, M. M., & Bailyn, C. D. 2004, ApJ, 615, 880
Cannizzo, J. K. 1993, ApJ, 419, 318
Cardelli, J. A., Clayton, G. C., & Mathis, J. S. 1989, ApJ, 345, 245
Casares, J. 2015, ApJ, 808, 80
Casares, J., & Charles, P. A. 1992, MNRAS, 255, 7
Casares, J., & Charles, P. A. 1994, MNRAS, 271, L5
Casares, J., Charles, P. A., Naylor, T., & Pavlenko, E. P. 1993, MNRAS, 265, 834
Coriat, M., Fender, R. P., & Dubus, G. 2012, MNRAS, 424, 1991
Dubus, G., Hameury, J.-M., & Lasota, J.-P. 2001, A&A, 373, 251
Hynes, R. I., Bradley, C. K., Rupen, M., et al. 2009, MNRAS, 399, 2239
Hynes, R. I., Charles, P. A., Garcia, M. R., et al. 2004, ApJL, 611, L125
Jain, R. K., Bailyn, C. D., Orosz, J. A., McClintock, J. E., & Remillard, R. A. 2001, ApJL, 554, L181
Khargharia, J., Froning, C. S., & Robinson, E. L. 2010, ApJ, 716, 1105
Kitamoto, S., Tsunemi, H., Miyamoto, S., Yamashita, K., & Mizobuchi, S. 1989, Natur, 342, 518
Krimm, H. A., Holland, S. T., Corbet, R. H. D., et al. 2013, yCat, 220, 90014
Kuulkers, E., Motta, S., Kajava, J., et al. 2015, ATel, 7647, 1
Lasota, J.-P. 2001, NewAR, 45, 449
Lasota, J.-P., Dubus, G., & Kruk, K. 2008, A&A, 486, 523
Lewis, F., Roche, P., Russell, D. M., & Fender, R. P. 2008, in AIP Conf. Proc. 1010, A Population Explosion: The Nature and Evolution of X-ray Binaries in Diverse Environments, ed. R. M. Bandyopadhyay et al. (Melville, NY: AIP), 204
Makino, F. 1989, IAUC, 4782, 1
Miller-Jones, J. C. A., Jonker, P. G., Dhawan, V., et al. 2009, ApJL, 706, L230
Muñoz-Darias, T., Sanchez, D. M., Casares, J., et al. 2015, ATel, 7659, 1
Narayan, R., Barret, D., & McClintock, J. E. 1997, ApJ, 482, 448
Narayan, R., & McClintock, J. E. 2008, NewAR, 51, 733
Narayan, R., McClintock, J. E., & Yi, I. 1996, ApJ, 457, 821
Oke, J. B. 1990, AJ, 99, 1621
Orosz, J. A., Remillard, R. A., Bailyn, C. D., & McClintock, J. E. 1997, ApJL, 478, L83
Rana, V., Loh, A., Corbel, S., et al. 2015, arXiv:1507.04049
Richter, G. A. 1989, IBVS, 3362, 1
Rodriguez, J., Cadolle Bel, M., Alfonso-Garzón, J., et al. 2015, A&A, 581, L9
Shahbaz, T., Bandyopadhyay, R. M., Charles, P. A., et al. 1998, MNRAS, 300, 1035
Shahbaz, T., Dhillon, V. S., Marsh, T. R., et al. 2003, MNRAS, 346, 1116
Smak, J. I. 1998, AcA, 48, 677
Terada, K., Miyamoto, S., Kitamoto, S., & Egoshi, W. 1994, PASJ, 46, 677
Udalski, A., & Kaluzny, J. 1991, PASP, 103, 198
Uemura, M., Kato, T., Matsumoto, K., et al. 2002, PASJ, 54, 285
Winkler, C., Courvoisier, T. J.-L., Di Cocco, G., et al. 2003, A&A, 411, L1
Wren, J., Akerlof, C., Balsano, R., et al. 2001, ApJL, 557, L97
Wu, J., Orosz, J. A., McClintock, J. E., et al. 2016, arXiv:1601.00616
Xie, F.-G., Yang, Q.-X., & Ma, R. 2014, MNRAS, 442, L110
Zurita, C., Casares, J., Hynes, R. I., et al. 2004, MNRAS, 352, 877
Zurita, C., Torres, M. A. P., Steeghs, D., et al. 2006, ApJ, 644, 432
Życki, P. T., Done, C., & Smith, D. A. 1999, MNRAS, 309, 561